Desalination and Water Treatment
www.deswater.com
doi: 10.1080/19443994.2015.1131199

57 (2016) 15676–15686
July

Taylor & Francis
Taylor & Francis Group

Application of cellulose acetate fibrous membranes in the removal of micro- and submicron solid particulates in drinking water media

Eisa A. Al Matroushi[a,*], Yaser E. Greish[b,*,1], Mohammed A. Meetani[b], Bothaina A. Al Shamisi[c]

[a]*Department of Chemical and Petroleum Engineering, College of Engineering, UAE University, Al Ain, P.O. Box 15551, United Arab Emirates, email: almatroushi@uaeu.ac.ae*
[b]*Department of Chemistry, College of Science, UAE University, Al Ain, P.O. Box 15551, United Arab Emirates, emails: y.afifi@uaeu.ac.ae (Y.E. Greish), mmeetani@uaeu.ac.ae (M.A. Meetani)*
[c]*Environment, Health and Safety Office, Al Ain Municipality, Al Ain, P.O. Box 1003, United Arab Emirates*

Received 2 September 2015; Accepted 4 December 2015

ABSTRACT

Cellulose is one of the most abundant natural polymers. Combined with its unique properties, cellulose nanofibers, therefore, have potential applications in industry. Electrospinning is a convenient technique that is widely used to make nanofibers. This process, however, needs optimization in order to fine tune the produced nanofibers. The current study investigates the effects of varying the different electrospinning parameters on the quality and monodispersity of the produced nanofibers. Cellulose acetate (CA), a cellulose precursor, is used in this regard. Solutions containing different concentrations of CA, up to 20% by weight, were electrospun into micro-nanofibers. The produced nanofibers were characterized by SEM, DSC, and IR techniques. Results showed the crucial dependence of the nanofibers monodispersity on the CA solution concentration, the applied voltage, the flow rate, the spinning distance, and the nature of atmosphere surrounding the electrospinning setup. Optimally prepared CA membranes as well as two commercially available filtering membranes were utilized in the removal of tiny solid particulates from drinking water media.

Keywords: Cellulose acetate; Electrospinning; Nanofibers; Solid particulates; Filtration

1. Introduction

In addition to common soluble pollutants in aqueous media, the presence of solid particulates in the range of micron–submicron size poses a deleterious effect on downstream membrane elements such as ultrafiltration and nanofiltration. These solid contaminants will tend to clog or foul membrane elements used in filtration processes, significantly decreasing the efficiency and output of the treatment [1]. There are various forms of pre-filters currently

*Corresponding authors.

[1]Permanent address: Department of Ceramics, National Research Center, Cairo, Egypt.

Presented at the 3rd International Conference on Water, Energy and Environment (ICWEE) 24–26 March 2015, Sharjah, United Arab Emirates

available such as packed sand beds, woven and non-woven fibrous meshes [2]. The choice of pre-filter is usually dictated by its properties, performance, and durability. A pre-filter should have an extremely large surface area, relating to high dirt-loading capacity. The smaller the fiber diameter used in the pre-filter, the greater the surface area for particle adsorption and the better the retention of small particles [1].

Polymeric nanofibrous membranes possess several characteristics that make them very attractive in separation technology, such as high porosity, pore sizes ranging from tens of nanometer to several micrometers, interconnected open pore structure, high permeability for gases, and a large surface area per unit volume [3]. Different techniques are used to make polymeric nanofibers [4–12]. The usefulness of these techniques is limited by combinations of restricted material ranges, possible fiber assembly, cost, and production rates [13]. Electrospinning is considered by many researchers the most convenient of these techniques, to make polymeric nanofibers [14–19]. It has received a significant interest as a simple, versatile, highly effective, and low-cost approach to produce nanofibers. In addition to the chemical properties of the polymer to be electrospun, studies have shown that the morphology and properties of the produced nanofibers are highly affected by the process parameters such as the operating voltage, type of solvent, concentration of the polymer solution, flow rate, spinning distance, needle gauge, and spinning atmosphere [18–21]. Nanofibers produced by electrospinning have shown great potential for a wide range of applications in healthcare, biotechnology, environmental engineering, defense, security, and energy generation. By having the ability to mass-produce nanofibers, electrospinning is highly believed to be one of the most significant nanotechnologies of this century [13].

Various polymers have been investigated for the manufacturing of micro- and nanofibrous filtration membranes [1,22]. Considering natural sources for the preparation of these membranes, cellulose could be considered a polymer with the highest potential in the field of filtration membranes [23,24]. Cellulose nanofibers can be extracted from plant or animal sources as well as fabricated using electrospinning technique. Cellulose fibers and whiskers have been recently used as reinforcing agents for nanocomposites with biomedical applications [25], and in combination with silica nanoparticles and polyamide-amine-epichlorohydrin (PAE) for filtration applications [26]. Non-traditional solvent systems are usually used in both approaches [27–33]. However, complete removal of these solvents cannot be achieved [34]. Alternatively, cellulose derivatives, such as cellulose acetate (CA), have been proposed due to the ease of their dissolution and their high electrospinnability [35–47]. Solutions of CA in different traditional mixed solvent systems, containing polar and non-polar solvents, were electrospun into nanofibers [47–53]. CA nanofibrous membranes exhibited high surface area and high porosity compared with common filter paper, and displayed high water permeability and a good hydrolytic stability. For the application of CA nanofibrous membranes in the removal of sub-micron size particulates, they must show a high degree of homogeneity in the fiber size and pore size distributions. This can be carried out through the optimization of the various electrospinning parameters. In the current article, the effects of varying the electrospinning parameters on the structural stability and homogeneity of the fiber size and pore size distributions of the nanofibrous membranes prepared, hereafter, were studied. Thereafter optimally prepared CA nanofibrous membranes were further evaluated for their ability to separate tiny solid particulates from drinking water. In comparison, two commercially available fibrous membranes were also evaluated.

2. Experimental work

CA used in the current study was obtained from Sigma–Aldrich, USA, with a 39.7 wt% acetyl content and an average M_n ca of 50,000 (by GPC); Fig. 1(a). Solvent system used to dissolve CA included N,N-dimethyl acetamide (DMAc), obtained as a ReagentPlus® with a min. assay of ≥99%, and acetone, that was purchased from Merck (Darmstadt, Germany) with a minimum assay of ≥99.8%. A solvent mixture containing acetone and DMAc (2:1 v/v) was prepared. Solutions containing 10, 12, 15, 17, and 20% (w/v) of CA were prepared by dissolving the appropriate amounts of CA powder in the solvent mixture warming at a temperature around 30–35˚C. The viscosity of each of these solutions was measured at ambient conditions using a Rheometer, Anton Paar (Austria), while the interfacial tensions were determined using a ring tensiometer. Results were processed using Rheolab plus software. For the purposes of this study, the shear-thinning behavior of CA as a non-Newtonian fluid was captured quantitatively by a power-law expression ($\eta = m\dot{\gamma}^{n-1}$, where η is viscosity in mPa s, $\dot{\gamma}$ is shear rate in s^{-1}, m is consistency index in mPa s, and n is flow behavior index).

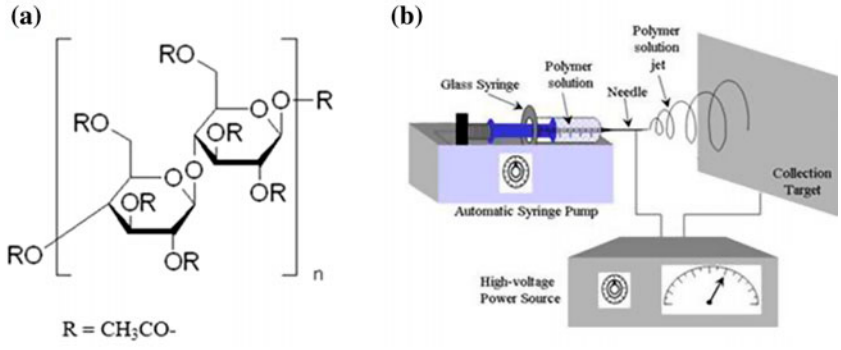

Fig. 1. Schematic diagram of (a) chemical structure of CA starting material and (b) electrospinning setup used for the preparation of the nanofibrous membranes.

To carry out the electrospinning experiment, a 5 mL volume of the polymer solution was placed into a plastic syringe with a metallic needle (gauge 18). A high voltage power supply (Gamma High Voltage Research, Florida-USA) and a vertical electrospinning setup was used; Fig. 1(b). Based on our previous findings, an optimum applied voltage of 12 kV was used throughout the study [54]. The effects of varying the initial concentration of the CA solutions, the rate of flow of the CA solution during spinning, and the spinning distance, on the homogeneity and size distribution of the obtained fibers, were investigated. Completely dry CA fibrous sheets were characterized for their composition by infrared spectroscopy (IR using a Nicolet Nexus 470 IR spectrosphotometer, USA) and differential scanning calorimeter (DSC 200F3–NETZSCH, Germany). Using the later technique, samples were heated at a rate of 20°C/min for a maximum temperature of 270°C. The morphology of the as-prepared fibrous membranes was studied using a scanning electron microscopy (Quanta inspect SEM, the Netherlands). N_2 adsorption studies at 77 K were conducted on a Quantochrome Autosorb-1 volumetric gas sorption instrument for the measurements of porosity and pore size distribution using the Barrett–Joyner–Halenda (BJH) model from the desorption branch of the N_2 isotherms. In order to evaluate the efficiency of the optimally prepared CA fibrous membrane for the removal of sub-micron size particulates from aqueous media, a simulated solid pollutant of hydroxyapatite ($Ca_{10}(PO_4)_6(OH)_2$; HAp), which has a K_{sp} value of 6.8×10^{-37}, obtained from Sigma–Aldrich, USA, with >99% purity, was used.

The powder sample contains a wide range of particle sizes (<1 to −12 μm), as derived from its SEM micrograph. A simulated deionized aqueous medium containing 300 ppm of HAp was used in the filtration experiment. Fig. 2 shows a schematic diagram of the experimental filtration setup that was used for evaluating the CA membranes for their efficiency in the removal of HAp particulates. Eq. (1) shows the % efficiency of HAp removal that was used in the study:

$$\text{Efficiency}\,(\%) = \left(\frac{X_o - X_i}{X_o}\right) \times 100 \quad (1)$$

where X_o is the initial concentration of Ca^{2+} ions, representing HAp in the deionized aqueous medium containing 300 ppm of HAp particulates, and X_i is the concentration of Ca^{2+} ions in the solution after filtration. Concentrations of Ca^{2+} ions were determined using an inductively coupled plasma-atomic emission spectroscopy (ICP-AES) technique. Measurements were done in triplicates, and an average value was used in the calculations of % efficiency. SEM micrographs of the CA membranes before and after filtration were recorded, while energy-dispersive X-ray (EDX) spectra were collected for the removed HAp particulates to ensure their composition. In all evaluation experiments, two commercially available filter membranes were used for comparison. These were made of various fibrous materials, silicates with various aspect ratios and polypropylene, and named hereafter as COM1 and COM2, respectively. Both optimally prepared nanofibrous CA and the commercial membranes were made into circular disks, 5 cm in diameter and 0.2 cm in thickness. Each disk was fixed inside the filtration cylinder using stainless steel washers (10 cm in external diameter, 8 cm internal diameter, and 0.2 c in thickness).

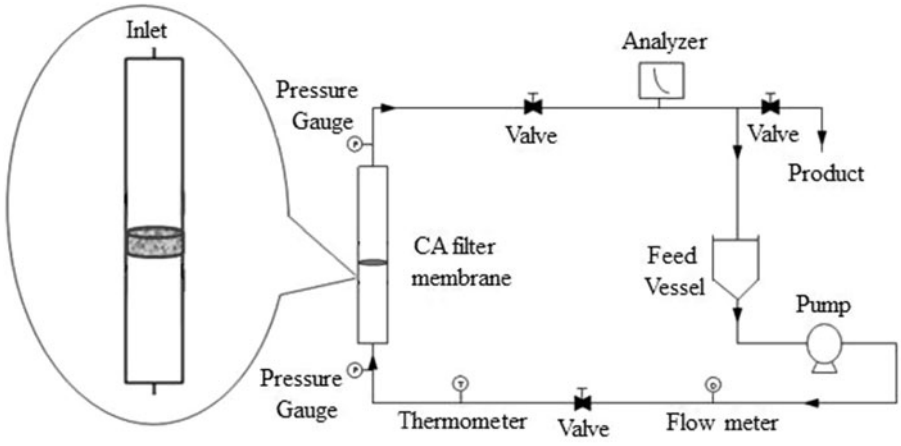

Fig. 2. Schematic diagram of the filtration setup used for the evaluation of CA membranes in the removal of solid particulates from simulated aqueous media. CA membranes were located inside the PVC pipes shown to the left side of the diagram.

3. Results and discussion

Solutions containing different concentrations of the same polymer are known to exhibit various degrees of viscosity, a physical property that is known to highly affect the formation of nanofibers by electrospinning. The flow of highly concentrated polymer solutions is different from those with lower concentrations, which is mainly attributed to the differences in their viscosities. Therefore, studying the rheological properties of the CA solutions prepared in the current study is highly important since the formation of polymer droplets as they emerge from the spinneret will highly depend on viscosity of their respective solutions, and is expected to affect the fiber diameter in the final web of nanofibers. The rheological properties of the solutions containing 10, 12, 15, 17, and 20 wt% of CA solutions were studied. Both viscosity and surface tension of these solutions were measured. Results of the modeling analysis are reported in Table 1 for values of m and n. The shear-dependent viscosities and shear stress of the CA solutions used in the experiments are shown in Fig. 3. Higher concentrations of CA fluids exhibited qualitatively similar (shear-thinning) viscous behavior as shown in Fig. 3(a). The CA-20 solution is highly elastic while the CA-10 solution is weakly elastic. The elastic nature of the CA solutions is demonstrated by the strain dependence of the shear shown in Fig. 3(b). The reduction in shear stress (at constant shear rate) increased with the increase in the CA concentration. Lower concentrations of CA (CA-10, CA-12) exhibited a constant slope, suggesting that these CA solutions behave as Newtonian fluids. The variation of the surface tension with CA concentration is shown in Table 1. The surface tension exhibited an increasing trend as a function of the CA concentration, showing a relatively higher increase at higher CA concentration.

Table 1
Physical properties of CA solutions used in the experiments

	Viscosity (mPa s)		
[CA] (w/v)	m	n	Surface tension (mN/m)
10	0.95	0.99	36.0
12	1.65	0.97	41.0
15	4.21	0.93	52.0
17	7.09	0.90	93.5
20	9.63	0.99	–[a]

[a]Could not be measured due to high viscosity of the solution.

At a constant electrospinning voltage of 12 kV solutions containing 10, 12, 15, 17, and 20 wt% of CA were electrospun at an arbitrary distance and flow rate of 14 cm and 100 mL/h, respectively. Fig. 4(a) shows the variation of fiber size distribution with varying the initial concentration of the CA solutions. These were measured from their corresponding SEM micrographs. It is evident that the fiber diameter increases as a result of increasing the concentration of CA in the original solutions, which is in accordance with the previous findings by Liu and Hsieh [55]. A maximum diameter of 1.8 mm was obtained from a solution containing 20 wt% of CA. It should be mentioned that it was relatively difficult to spin the CA solution containing 20 wt% and beyond because of its relatively higher viscosity. The least average fiber diameter of

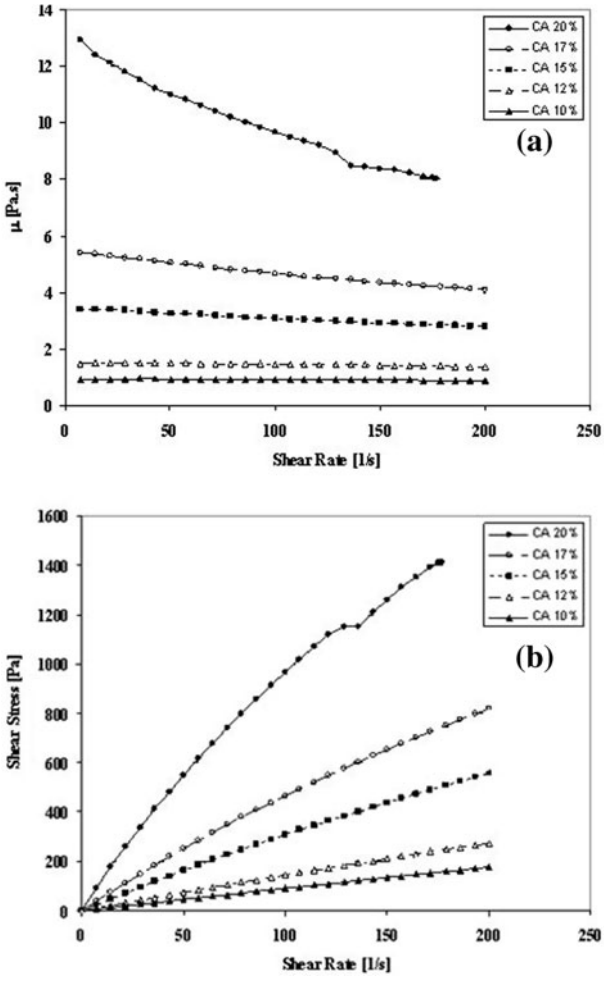

Fig. 3. Viscosity (a) and shear stress (b) curves of solutions containing 10, 12, 15, 17, and 20 wt% of cellulose in acetone: DMAc (2:1) solvent mixture, as a function of shear rate (n = 3).

around 380 nm was obtained from solution containing 12 wt% of CA. This solution was previously shown to behave as a Newtonian fluid, Fig. 3, a solution containing 12 wt% of CA was electrospun at an operating voltage of 12 kV, distance of 14 cm, and a flow rate of 5, 10, 15, 20, 25, 50, and 100 mL/hr. Fig. 4(b) shows the average fiber size distribution as a function of the flow rate. Previous findings by Megelski et al. showed that the increase of fiber diameter with increasing the rate of polymer flow [56]. They found that at very high flow rates, fibers had pronounced beaded morphologies [56]. Based on these findings, a high flow rate of 100 mL/h was avoided in our experiments since similar beaded morphologies were obtained. At a lower flow rate, 50 mL/h, fibers with a ribbon-like morphology were produced. At lower flow rates,

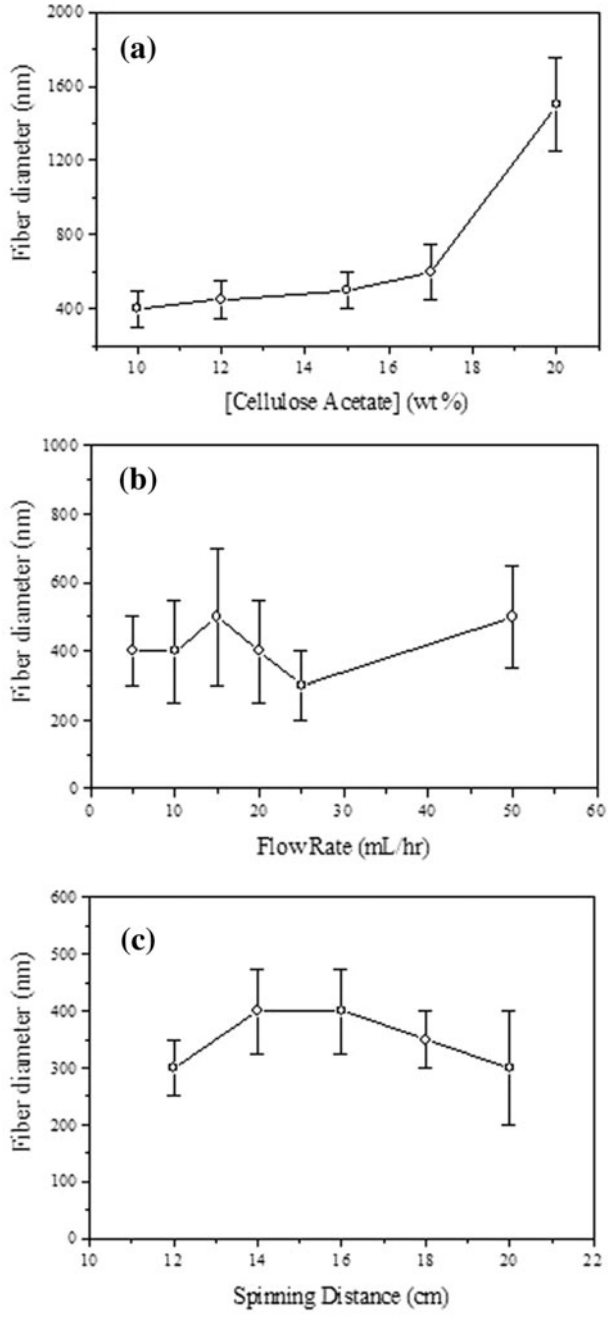

Fig. 4. Average fiber size distribution of CA fibrous membranes obtained by electrospinning CA solutions in acetone: DMAc (2:1) solvent mixture at a constant voltage of 12 kV, and as a function of cellulose concentration (a), flow rate (b), and spinning distance (c) (n = 3).

beads-free nanofibers were produced with a fiber diameter increasing with increasing the flow rate. However, membranes produced at a flow rate of 5 mL/h had the highest homogeneity throughout the membrane, as shown in Fig. 5(a). The least fiber

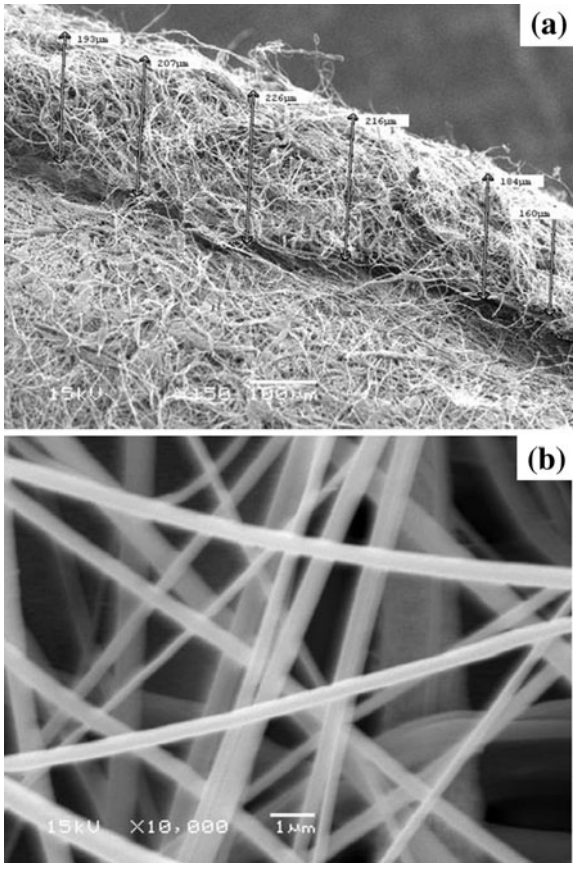

Fig. 5. Scanning electron micrographs of optimally prepared CA nanofibrous membrane (a) from a 12 wt% solution of CA in acetone: DMAc (2:1) solvent mixture, using a constant voltage of 12 kV, a flow rate of 5 ml/hr, and a spinning distance of 14 cm and (b) shows a high magnification of the same fibrous membrane showing its uniform size distribution.

diameter obtained at this low flow rate was 380 nm, which is also the least among all membranes obtained at different flow rates. The homogeneous fiber size distribution shown in Fig. 4(b) indicates a homogeneous pore size distribution, a characteristic that is advantageous for environmental applications of these membranes.

The structure and morphology of electrospun fibers is easily affected by the nozzle to collector distance because of their dependence on the deposition time, evaporation rate, as well as the whipping or instability interval during the fibers deposition on the collector [2]. Therefore, the effect of varying the nozzle to collector distance between 12 and 20 cm (step 2 cm) was studied during the spinning of a solution containing 12 wt% CA at a constant operating voltage of 12 kV, and a constant flow rate of 5 mL/h. Fig. 4(c) shows the average fiber size distribution of fibers obtained at fixed spinning voltage and flow rate and variable spinning distances. Despite the fact that at a spinning distance of 14 cm, fibers with higher average size were obtained, this distance was found optimum where non-fibrous morphologies were obtained at other spinning distances. Fig. 5 shows SEM micrographs at various magnifications of optimally prepared CA fibrous membrane. It should be mentioned that the presence of a distribution of the fiber sizes provides different extents of interconnected porosities as a result of the non-woven nature of the fibrous membrane. These porosities are, therefore, considered advantageous since solid particulates of various sizes can be removed. Based on these results, optimally prepared fibrous membranes were subjected to measurement of their pore size distribution using N_2-adsorption. Fig. 6 shows pore size distribution of an optimally prepared CA fibrous membrane. A variable size distribution ranging from (I) microporous (<2 nm), to (II) mesoporous (2–50 nm) to (III) macroporous (>50 nm) was observed [57]. With the presence of these types of porosities, these fibrous membranes are proven to have interconnected porosities of various extents, as shown in Fig. 5(b); membranes with different extents of porosities are more suitable for the capture of various sizes of solid particulates and recommend them for filtration applications.

Optimally prepared electrospun CA nanofibrous were further investigated by IR and DSC techniques to ensure their structural stability as a result of electrospinning. Results were compared with the as-received CA powders. Results are shown in Fig. 7. The IR spectrum of the as-received CA, shown in Fig. 7(a) indicates its initial phase purity. Bands at different positions in the spectrum were interpreted by comparing the positions at which different functional groups in the CA absorb with their corresponding data obtained from the literature [58]. The presence of the acetate groups in the structure of CA was confirmed by locating the acetyl carbonyl (C=O) group at 1,760 cm^{-1}. The commercially supplied CA is known to contain 39.7 wt% as acetyl content. CA is also known as cellulose triacetate, considering substitution of the three hydroxyl (–OH) groups in cellulose by acetate. The presence of a broad band at 3,600–3,200 cm^{-1}, which denotes the O–H stretching mode, confirms the partial substitution of the OH groups in the original cellulose structure. However, the uniformity of substitution, and the presence of this percentage of acetate groups in the structure of CA could not be confirmed by IR. A close match can be seen between the spectra of both samples, before and after electrospinning. This indicates the

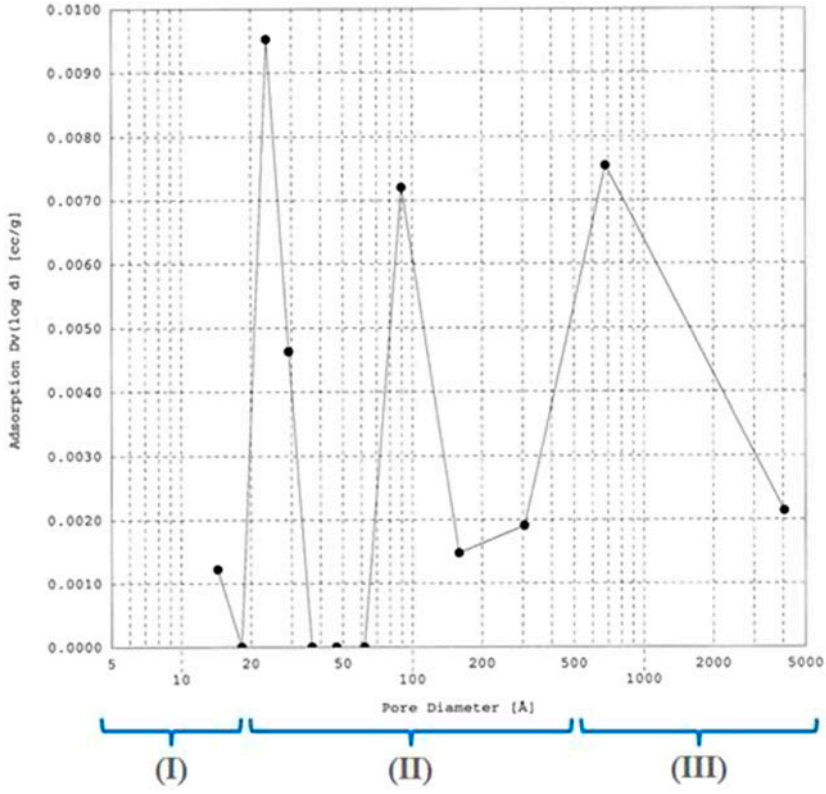

Fig. 6. Pore size distribution of an optimally prepared CA fibrous membrane as depicted from the N_2 adsorption measurements. Peaks denote the presence of different degrees of porosities (micro, meso, and macroporous) as a result of the non-woven nature of the membrane and the fiber size distribution [57].

structural stability of CA. Fig. 7(b) shows the DSC spectra of the as-spun versus the as-received CA samples, both heated up to 270°C. The glass transition (T_g) and melting (T_m) temperatures of CA are known to be around 198–205°C and 224–230°C, respectively [59]. The glass transition temperature of the as-received CA was calculated to be around 180°C. Fig. 7(b) shows two endotherms with peak temperatures of 107.2 and 236.1°C, respectively, in the graph of the as-received CA sample. The first broad endotherm is attributed to the evolution of water vapor, which is strongly adsorbed on the CA powder by hydrogen-bonding. The second endotherm may be attributed to melting temperature (T_m) of CA. Thermal results of CA thus confirm its structure. Thermal treatment of CA nanofibers was previously recommended in order to confirm the removal of remaining solvents and improve the mechanical integrity of the membranes [54]. The current results suggest a temperature range for thermal treatment of CA to be within a range of >180 to <236°C to avoid degradation of CA. DSC of the as-electrospun CA membrane indicates the absence of the dehydration endotherm. This is attributed to the evolution of all water of hydration as a result of drying these membranes at 100°C for 24 h before carrying out its DSC testing. A couple of endotherms were observed between 190 and 235°C. The last endotherm, at 230°C, is attributed to the melting temperature (T_m) of CA nanofibers, which is in accordance with that observed for as-received CA. The three endotherms at 190, 208, and 215°C are, therefore, attributed to a series of events taking place at these temperatures before melting of the fibers. These events were explained in terms of the gradual removal of the acetyl groups of the CA nanofibers [54]. A glass transition temperature (T_g) of around 186°C was calculated for the as-electrospun CA sample, which is slightly higher than that of the as-received CA shown in Fig. 7(b). A final conclusion in this respect is the absence of any thermal events at temperatures below 186°C, indicating its expected stability up to this temperature. In fact, at temperatures below the melting temperature of CA, the chemical structure stability of CA is presumably constant.

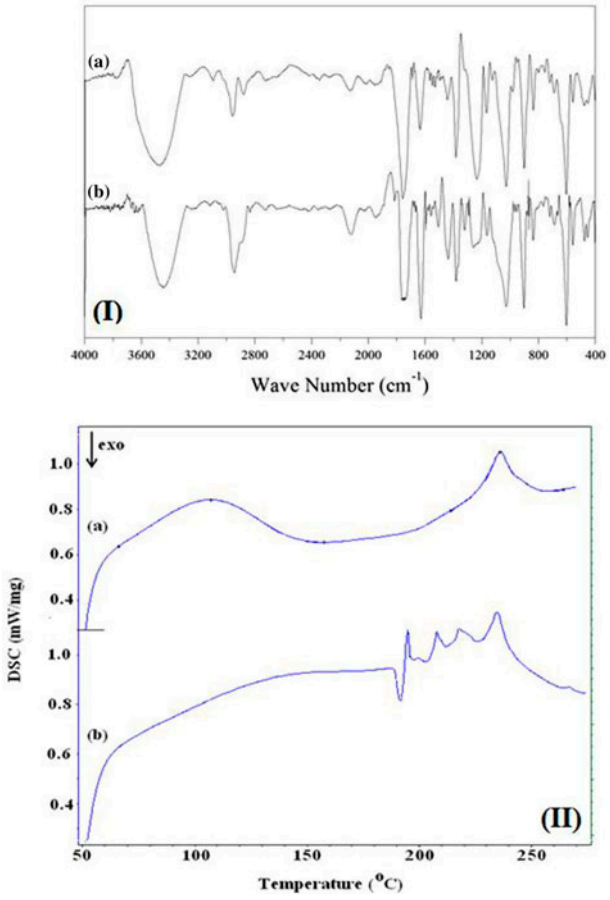

Fig. 7. Infrared spectrum (I) and differential scanning calorimetry diagram (II) of (a) as-received CA powder and (b) optimally prepared electrospun nanofibrous CA membrane, showing structural stability of the electrospun CA.

Evaluation of the performance of optimally prepared CA fibrous membranes for the removal of tiny (sub-micron size) solid particulates from drinking water was carried out in comparison with two commercially available water membrane. Fig. 8(a) and (b) shows SEM micrographs of the commercial filter membranes. These were obtained from the market and were identified as manufactured from silicate-based and polypropylene-based materials. Both membranes show a degree of interconnected porosity with variable size distribution, unlike the characteristics of the optimally prepared CA fibrous membrane. Fig. 9(c) shows SEM micrograph of the particulate HAp powder used in the filtration experiment. It shows a particle size range of <1–12 μm. Fig. 9 shows SEM micrographs of the three fibrous membranes after the removal of solid particulates from drinking water. To confirm the composition of the separated solid

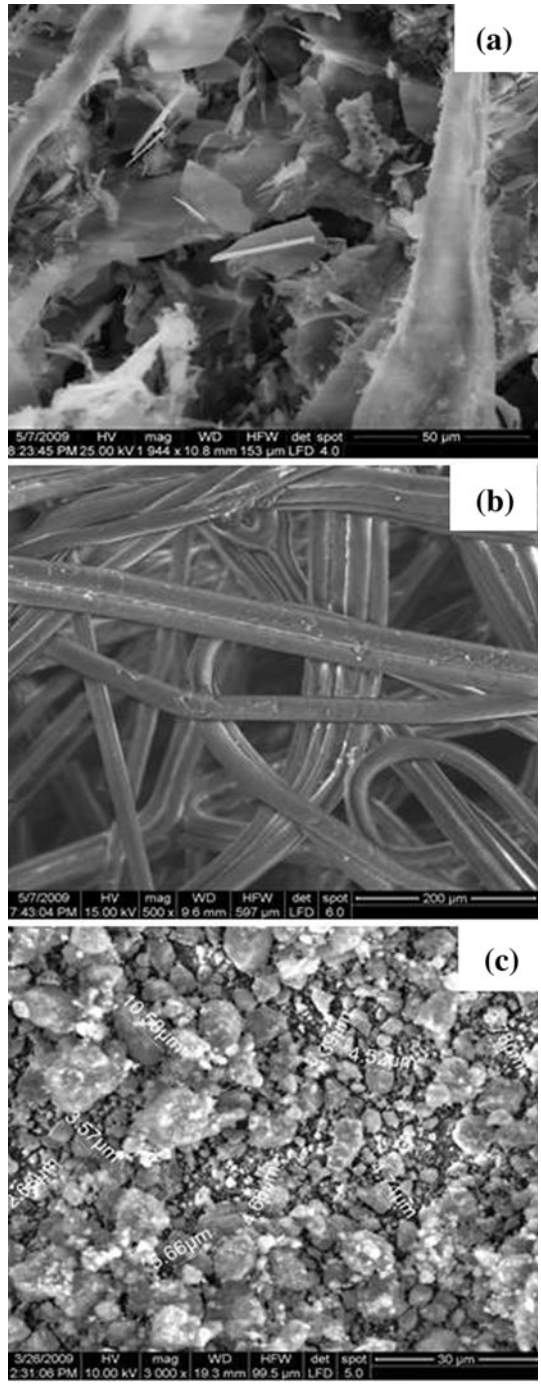

Fig. 8. Scanning electron micrographs of commercially available water filtration membranes; (a) silicate-based fibrous membrane (COM1); (b) polypropylene fibrous membrane (COM2), both used for comparison with the optimally prepared CA membrane for their efficiencies in the removal of solid particulates from aqueous media; and (c) calcium phosphate (hydroxyapatite) solid particulate pollutant sample used to simulate insoluble solid pollutants in aqueous media.

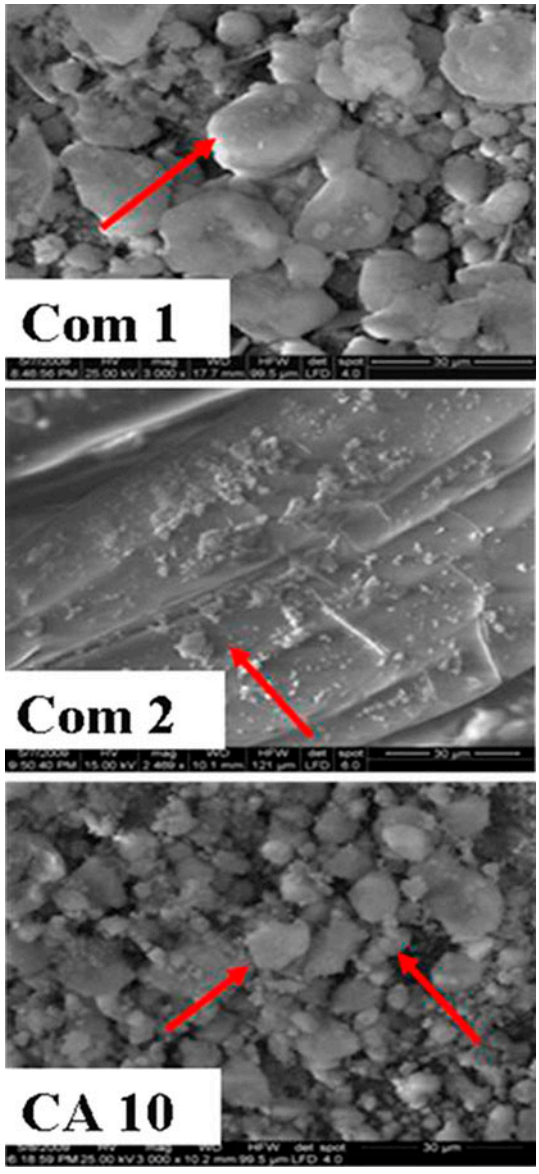

Fig. 9. Scanning electron micrographs of commercially membranes (COM1 and COM2) and the optimally prepared CA fibrous membranes (CA10) after the removal of solid particulates from aqueous media initially containing 300 ppm of the solid particulates. Solid particulates of various sizes are shown onto the CA10 membrane as compared with the commercial membranes.

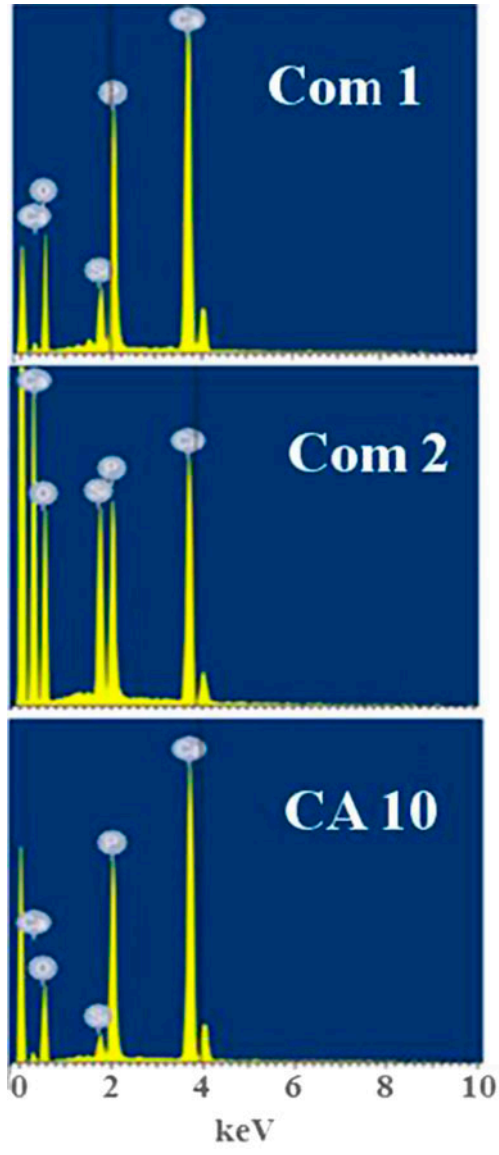

Fig. 10. EDX spectra confirming the composition of the solid particulates separated onto commercial (COM1 and COM2) and optimally prepared (CA10) membranes. Peaks representing Ca, P, and O are shown in all EDX spectra.

particulates, EDX analysis was performed, Fig. 10. All membranes were proven suitable for the removal of the solid particulates. The percentage removal of COM1 filter membrane was shown to be the highest, achieving 98%, while COM2 filter membrane showed a removal efficiency of 90%. In comparison, the optimally prepared CA fibrous membrane showed a removal efficiency of 95%. The high efficiency of the COM1 membrane could be attributed to the interlocking between the different morphologies of fibrous and non-fibrous constituents shown in Fig. 8(a). However, it should be mentioned that this membrane was not stable under continued water flow conditions where signs of mechanical degradation of the membrane were observed. In contrast, the low efficiency of the COM2 membrane is attributed to the lower surface area, higher size distribution, of the fibers comprising the filter membrane. These results, therefore, indicate the high potential of the optimally prepared CA fibrous membrane for the suggested application.

4. Conclusions

An electrospinning technique was used to prepare CA nanofibers. Optimization of the electrospinning parameters was carried. Acetone-DMAc as a common solvent system was used to make the CA solutions. Results, in general, showed the high dependence of the quality of the produced nanofibers on the CA solution concentration, the applied voltage, the flow rate, the spinning distance, and the nature of atmosphere surrounding the electrospinning setup. Highly concentrated CA solutions (≥17 wt%) were found relatively difficult to spin due to its high viscosity, where the produced nanofibers were relatively thicker than those obtained from CA solutions with lower concentrations using an optimum applied voltage of 12 kV. Lower flow rates of around 5 mL/h and a spinning distance of 14 cm were also found optimum for the production of thin, beads-free nanofibers. Fibers within a range of 200–400 nm were successfully obtained at these optimized conditions. These fibers showed structural and thermal stabilities and were shown superior over two commercially available fibrous membranes achieving a high efficiency of removal of solid particulates from drinking water media.

References

[1] D. Aussawasathien, C. Teerawattananon, A. Vongachariya, Separation of micron to sub-micron particles from water: Electrospun nylon-6 nanofibrous membranes as pre-filters, J. Membr. Sci. 315 (2008) 11–19.

[2] R.J. Akers, A.S. Ward, in: C. Orr (Ed.), Liquid Filtration Theory and Filtration Pretreatment, Filtration: Principles and Practices, Part I, Marcel Dekker, New York, NY, 1981, pp. 169–250.

[3] R. Gopal, S. Kaur, Z. Ma, C. Chan, S. Ramakrishna, T. Matsuura, Electrospun nanofibrous filtration membrane, J. Membr. Sci. 281 (2006) 581–586.

[4] T. Ondarçuhu, C. Joachim, Drawing a single nanofiber over hundreds of microns, Europhys. Lett. 42 (1998) 215–220.

[5] J. Feng, The stretching of an electrified non-Newtonian jet: A model for electrospinning, Phys. Fluids 14 (2002) 3912–3926.

[6] P.X. Ma, R. Zhang, Synthetic nano-scale fibrous extracellular matrix, J. Biomed. Mater. Res. 46 (1999) 60–72.

[7] M. Perez. Microfibers and method of making, US Patent 6, 110, 588, 2000.

[8] R. Pike. Superfine microfiber nonwoven web, US Patent 5, 935, 883, 1999

[9] D. Reneker. Process and apparatus for the production of nanofibers, US Patent 6, 382, 526, 2002

[10] A. Tseng, A. Notargiacomo, T. Chen, Nanofabrication by scanning probe microscope lithography: A review, J. Vac. Sci. Technol., B: Microelectron. Nanometer Struct. 23 (2005) 877–894.

[11] J. Huie, Guided molecular self-assembly: A review of recent efforts, Smart Mater. Struct. 12 (2003) 264–271.

[12] E. Luong-Van, L. Grøndahl, K. Chua, K. Leong, V. Nurcombe, S. Cool, Controlled release of heparin from poly(ε-caprolactone) electrospun fibers, Biomaterials 27 (2006) 2042–2050.

[13] S. Ramakrishna, K. Fujihara, W. Teo, T. Yong, Z. Ma, Yong, Z. Ma, R. Ramaseshan. Electrospun nanofibers: Solving global issues, Mater. Today 9 (2006) 40–50.

[14] Q. Yu, M. Shi, M. Deng, M. Wang, H. Chen, Morphology and conductivity of polyaniline sub-micron fibers prepared by electrospinning. Mater. Sci. Eng. B 150 (2008) 70–76

[15] D. Li, Y. Xia, Electrospinning of nanofibers: Reinventing the wheel? Adv. Mater. 16 (2004) 1151–1170.

[16] H. Pan, L. Li, L. Hu, X. Cui, Continuous aligned polymer fibers produced by a modified electrospinning method, Polymer 47 (2006) 4901–4904.

[17] J. Deitzel, W. Kosik, S. McKnight, N. Tan, J. DeSimone, S. Crette, Electrospinning of polymer nanofibers with specific surface chemistry, Polymer 43 (2002) 1025–1029.

[18] J. Deitzel, J. Kleinmeyer, D. Harris, N.C. Beck Tan, The effect of processing variables on the morphology of electrospun nanofibers and textiles, Polymer 42 (2001) 261–272.

[19] G. Rutledge, S. Fridrikh, Formation of fibers by electrospinning, Adv. Drug Delivery Rev. 59 (2007) 1384–1391.

[20] S. Ramakrishna, K. Fujihara, W. Teo, T. Lim, Z. Ma, An Introduction to Electrospinning and Nanofibers, World Scientific Publishing Co., Singapore, 2005.

[21] A. Frenot, I.S. Chronakis, Polymer nanofibers assembled by electrospinning, Curr. Opin. Colloid Interface Sci. 8 (2003) 64–75.

[22] R. Gopal, S. Kaur, C. Feng, C. Chan, S. Ramakrishna, S. Tabe, T. Matsuura, Electrospun nanofibrous polysulfone membranes as pre-filters: Particulate removal, J. Membr. Sci. 289 (2007) 210–219.

[23] S. Kaur, Z. Ma, C. Chan, S. Ramakrishna, T. Matsuura, Electrospun nanofibrous filtration membrane, J. Membr. Sci. 281 (2006) 581–586.

[24] H. Abdul Khalil, A. Bhat, A. Ireana Yusra. Green composites from sustainable cellulose nanofibrils: A review. Carbohydr. Polym.87 (2012) 963–979

[25] M. Mounika, K. Ravindra, Characterization of Nanocomposites Reinforced with Cellulose Whiskers: A Review, Mater. Today: Proc. 2 (2015) 3610–3618.

[26] S. Varanasi, Z. Low, W. Batchelor, Cellulose nanofibre composite membranes—Biodegradable and recyclable UF membranes, Chem. Eng. J. 265 (2015) 138–146.

[27] H. Ma, C. Burger, B. Hsiao, B. Chu, Fabrication and characterization of cellulose nanofiber based thin-film nanofibrous composite membranes, J. Membr. Sci. 454 (2014) 272–282.

[28] C. Kim, D. Kim, S. Kang, M. Marquez, Y. Joo, Structural studies of electrospun cellulose nanofibers, Polymer 47 (2006) 5097–5107.

[29] S. Xu, J. Zhang, A. He, J. Li, H. Zhang, C. Han, Electrospinning of native cellulose from nonvolatile solvent system, Polymer 49 (2008) 2911–2917.

[30] C. Kim, M. Frey, M. Marquez, Y. Joo, Preparation of submicron-scale, electrospun cellulose fibers via direct dissolution, J. Polym. Sci. Part B: Polym. Phys. 43 (2005) 1673–1683.

[31] P. Kulpinski, Electrospinning of cellulose-based nanofibers, J. Appl. Polym. Sci. 98 (2005) 1473–1482.
[32] S. Han, W. Son, J. Youk, W. Park, Electrospinning of ultrafine cellulose fibers and fabrication of poly(butylene succinate) biocomposites reinforced by them, J. Appl. Polym. Sci. 107 (2008) 1954–1959.
[33] L. Zhang, T. Menkhaus, H. Fong, Fabrication and bioseparation studies of adsorptive membranes/felts made from electrospun cellulose acetate nanofibers, J. Membr. Sci. 319 (2008) 176–184.
[34] M. Frey, Electrospinning of cellulose and cellulose derivatives, Polym. Rev. 48 (2008) 378–391.
[35] H. Liu, Y. Hsieh, Surface methacrylation and graft copolymerization of ultrafine cellulose fibers, J. Polym. Sci. Part B: Polym. Phys. 41 (2003) 953–964.
[36] W. Son, J. Youk, T. Lee, W. Park, Electrospinning of ultrafine cellulose acetate fibers: Studies of a new solvent system and deacetylation of ultrafine cellulose acetate fibers, J. Polym. Sci. Part B: Polym. Phys. 42 (2004) 5–11.
[37] S. Tungprapa, T. Puangparn, M. Weerasombut, I. Jangchud, P. Fakum, S. Semongkhol, C. Meechaisue, P. Supaphol, Electrospun cellulose acetate fibers: Effect of solvent system on morphology and fiber diameter, Cellulose 14 (2007) 563–575.
[38] S. Han, J. Youk, K. Min, Y. Kang, W. Park, Electrospinning of cellulose acetate nanofibers using a mixed solvent of acetic acid/water: Effects of solvent composition on the fiber diameter, Mater. Lett. 62 (2008) 759–762.
[39] S. Han, W. Son, J. Youk, T. Lee, W. Park, Ultrafine porous fibers electrospun from cellulose triacetate, Mater. Lett. 59 (2005) 2998–3001.
[40] M. Wang, L. Wang, Y. Huang, Electrospun hydroxypropyl methyl cellulose phthalate (HPMCP)/erythromycin fibers for targeted release in intestine, J. Appl. Polym. Sci. 106 (2007) 2177–2184.
[41] X. Wu, L. Wang, H. Yu, Y. Huang, Effect of solvent on morphology of electrospinning ethyl cellulose fibers, J. Appl. Polym. Sci. 97 (2005) 1292–1297.
[42] J. Park, S. Han, I. Lee, Preparation of electrospun porous ethyl cellulose fiber by THF/DMAc binary solvent system, J. Ind. Eng. Chem. 13 (2007) 1002–1008.
[43] A. Frenot, M. Henriksson, P. Walkenström, Electrospinning of cellulose-based nanofibers, J. Appl. Polym. Sci. 103 (2007) 1473–1482.
[44] S. Zhao, X. Wu, L. Wang, Y. Huang, Electrospinning of ethyl-cyanoethyl cellulose/tetrahydrofuran solutions, J. Appl. Polym. Sci. 91 (2004) 242–246.
[45] S. Zhao, X. Wu, L. Wang, Y. Huang, Electrostatically generated fibers of ethyl-cyanoethyl cellulose, Cellulose 10 (2003) 405–409.
[46] N. Abdelwahab, N. Ammar, H. Ibrahim, Graft copolymerization of cellulose acetate for removal and recovery of lead ions from wastewater, Int. J. Biol. Macromol. 79 (2015) 913–922.
[47] T. Lan, Z. Shao, M. Gu, Z. Zhou, Y. Wang, W. Wang, F. Wang, J. Wang, Electrospun nanofibrous cellulose diacetate nitrate membrane for protein separation, J. Membr. Sci. 489 (2015) 204–211.
[48] H. Liu, Y. Hsieh, Ultrafine fibrous cellulose membranes from electrospinning of cellulose acetate, J. Polym. Sci. Part B: Polym. Phys. 40 (2002) 2119–2129.
[49] P. Lu, Y. Hsieh, Lipase bound cellulose nanofibrous membrane via Cibacron Blue F3GA affinity ligand, J. Membr. Sci. 330 (2009) 288–296.
[50] W. Ritcharoen, P. Supaphol, P. Pavasant, Development of polyelectrolyte multilayer-coated electrospun cellulose acetate fiber mat as composite membranes, Eur. Polym. J. 44 (2008) 3963–3968.
[51] Y. Yoon, H. Moon, W. Lyoo, T. Lee, W. Park, Superhydrophobicity of cellulose triacetate fibrous mats produced by electrospinning and plasma treatment, Carbohydr. Polym. 75 (2009) 246–250.
[52] Z. Ma, S. Ramakrishna, Electrospun regenerated cellulose nanofiber affinity membrane functionalized with protein A/G for IgG purification, J. Membr. Sci. 319 (2008) 23–28.
[53] L. Chen, L. Bromberg, T. Hatton, G. Rutledge, Electrospun cellulose acetate fibers containing chlorhexidine as a bactericide, Polymer 49 (2008) 1266–1275.
[54] Y. Greish, M. Meetani, E. Al Matroushi, B. Al Shamsi, Effects of thermal and chemical treatments on the structural stability of cellulose acetate nanofibers, Carbohydr. Polym. 82 (2010) 569–577
[55] H. Liu, Y. Hsieh, Ultrafine fibrous cellulose membranes from electrospinning of cellulose acetate, J. Polym. Sci. Part B: Polym. Phys. 40 (2002) 2119–2129.
[56] S. Megelski, J. Stephens, D. Chase, J. Rabolt, Micro- and nanostructured surface morphology on electrospun polymer fibers, Macromolecules 35 (2002) 8456–8466.
[57] F. Rouquerol, K. Sing, Adsorption by Powders and Porous Solids: Principles, Methodology and Applications, Academic Press, UK, 1999.
[58] D. Skoog, F. Holler, T. Nieman, Principles of Instrumental Analysis, fifth ed., Thomson Learning, USA, 1998.
[59] M. Meier, L. Kanis, V. Soldi, Characterization and drug-permeation profiles of microporous and dense cellulose acetate membranes: Influence of plasticizer and pore forming agent, Int. J. Pharm. 278 (2004) 99–110.